

# Heme Oxygenase-1 Inhibits Pro-Oxidant Induced Hypertrophy in HL-1 Cardiomyocytes

KEITH R. BRUNT,\* MATTHEW R. TSUJI,\* JOYCE H. LAI,\* ROBERT T. KINOBE,\*  
WILLIAM DURANTE,† WILLIAM C. CLAYCOMB,‡ CHRISTOPHER A. WARD,\*<sup>1</sup> AND  
LUIS G. MELO\*<sup>2</sup>

\*Department of Physiology, Queen's University, Kingston, Ontario, K7L 3N6 Canada; †Department of Medical Pharmacology and Physiology, University of Missouri, Columbia, Missouri 65212; and ‡Department of Biochemistry and Molecular Biology, Louisiana State University, Health Sciences Center, New Orleans, Louisiana 70112-1394

**Aims:** Reactive oxygen species (ROS) activate multiple signaling pathways involved in cardiac hypertrophy. Since HO-1 exerts potent antioxidant effects, we hypothesized that this enzyme inhibits ROS-induced cardiomyocyte hypertrophy. **Methods:** HL-1 cardiomyocytes were transduced with an adenovirus constitutively expressing HO-1 (AdHO-1) to increase basal HO-1 expression and then exposed to 200  $\mu$ M hydrogen peroxide ( $H_2O_2$ ). Hypertrophy was measured using  $^3H$ -leucine incorporation, planar morphometry and cell-size by forward-scatter flow-cytometry. The pro-oxidant effect of  $H_2O_2$  was assessed by redox sensitive fluorophores. Inducing intracellular redox imbalance resulted in cardiomyocyte hypertrophy through transactivation of nuclear factor kappa B (NF- $\kappa$ B). **Results:** Pre-emptive HO-1 overexpression attenuated the redox imbalance and reduced hypertrophic indices. This is the first time that HO-1 has directly been shown to inhibit oxidant-induced cardiomyocyte hypertrophy by a NF- $\kappa$ B-dependent mechanism. **Conclusion:** These results demonstrate that HO-1 inhibits pro-oxidant induced cardiomyocyte hypertrophy and suggest that HO-1 may yield therapeutic potential in treatment of

cardiac hypertrophy and prevention of heart failure. *Exp Biol Med* 234:582–594, 2009

**Key words:** NF- $\kappa$ B; adenovirus; heme; carbon monoxide; bilirubin; oxidative stress

## Introduction

Cardiomyocyte hypertrophy usually develops as an adaptive response to conditions that lead to chronic hemodynamic overload, such as hypertension and valvular disease (1, 2). However, in time, the increase in myocyte size eventually leads to contractile dysfunction, culminating in heart failure and death (1). Several lines of evidence suggest that redox imbalance plays an essential role in cardiomyocyte hypertrophy and heart failure (3–5). Reactive oxygen species (ROS) generation is increased in hypertrophied hearts in response to mechanical stretch and cytokine stimulation (4, 6), with antioxidants reportedly preventing the development of heart failure in animals with chronic pressure overload (7–9). Furthermore, ROS activate pro-hypertrophic signaling cascades and induce hypertrophy in isolated myocytes (10–15, for reviews see 16, 17), in part through NF- $\kappa$ B mechanisms (13). Indeed, genetic blockade of NF- $\kappa$ B, a redox sensitive transcription factor, reduces myocardial hypertrophy without deteriorating cardiac function (18). Though perhaps most convincingly, Yamamoto et al (19) showed that transgenic mice overexpressing a dominant negative mutant of the antioxidant enzyme thioredoxin have marked cardiac hypertrophy in association with increased oxidative stress. Thus, oxidative stress, regardless of intrinsic or extrinsic source of induction, affects redox sensitive mechanisms regulating hypertrophy.

Heme oxygenase-1 (HO-1) is a ubiquitously expressed stress inducible enzyme that catabolizes heme into bilirubin, carbon monoxide (CO) and iron (20). The by-products of heme catabolism exert pleiotropic cytoprotective effects in the heart. Bilirubin is a powerful antioxidant (21), and CO

---

This work was supported by grants from the Canadian Institutes of Health Research (CIHR, MOP 79506) and the Heart and Stroke Foundation of Ontario (HSFO, NA 5779) to L. G. M. and C. A. W. W. D. is supported by a grant from the National Institute of Health (NIH, HL59976). K. R. B. is supported by a doctoral award from Canadian Institute of Health Research/Heart & Stroke Foundation G.R.E.A.T. training program. R. K. is supported by a postdoctoral fellowship from the Heart and Stroke Foundation of Canada. L. G. M. was a Canada Research Chair in Molecular Cardiology and a New Investigator of the Heart and Stroke Foundation of Canada.

---

<sup>1</sup> To whom correspondence should be addressed at Department of Physiology, Queen's University, 431 Botterell Hall, Kingston, Ontario K7L 3N6, Canada. E-mail: wardc@queensu.ca

---

<sup>2</sup> Deceased.

---

Received October 30, 2008.  
Accepted January 26, 2009.

---

DOI: 10.3181/0810-RM-312  
1535-3702/09/2345-0582\$15.00  
Copyright © 2009 by the Society for Experimental Biology and Medicine

exerts vasodilatory, anti-inflammatory and anti-proliferative effects (22). HO-1 is upregulated in a number of disease states characterized by oxidative stress, including myocardial ischemia and cardiac hypertrophy (8, 23), and exogenous HO-1 overexpression decreases ROS production in ischemic myocardium (24, 25). Others have shown that HO-1 overexpression using adenovirus decreases agonist-induced cardiomyocyte hypertrophy by inhibiting mechanisms such as Erk 1/2, p38 and calcineurin/NFAT (26).

Furthermore, Hu et al (27) showed recently that angiotensin-II-induced cardiac hypertrophy was decreased by HO-1 in association with a decrease in oxidative stress; however, this finding appears to be equivocal because, in a recent study, Foo et al (28) reported that HO-1 failed to inhibit angiotensin-II-induced hypertrophy. Thus, these findings suggest HO-1 may be a novel negative regulator of cardiac growth that may function as a compensatory mechanism against ROS-induced cardiac hypertrophy, but agonist-induced hypertrophy may produce equivocal results. A direct role of HO-1 in inhibiting oxidative stress-induced cardiomyocyte hypertrophy has not yet been examined.

In the current study, we investigated the effect of HO-1 on oxidant-induced hypertrophy in the HL-1 cardiomyocyte cell-line, which shares immunohistochemical, electrophysiological and pharmacological properties of adult myocytes, including the presence of organized sarcomeres, and the ability to spontaneously depolarize and generate action potentials in response to inotropic and chronotropic agonists (29, for review 30). In addition, these cardiomyocytes have abundant atrial natriuretic factor-containing granules and exhibit a gene expression profile similar to adult primary cardiomyocytes (29). Though established as a cardiomyocyte line for study of electrical, metabolic and signaling alterations in pathological conditions, such as hypoxia, hyperglycemia and ischemia-reperfusion injury (30, 31, 32), the use of HL-1 as a model to study cardiac hypertrophy is rare (33). Part of our objective is to affirm that the HL-1 cardiomyocytes are a homogenous, congruous and cost effective model to study the molecular mechanisms of cardiac hypertrophy. Our current findings show that HO-1 markedly reduces oxidant-induced hypertrophy in HL-1 cardiomyocytes, supporting the premise that HO-1 is a novel negative regulator of oxidant-induced cardiac hypertrophy.

## Materials and Methods

**Reagents.** Claycomb medium and fetal bovine serum (FBS) were purchased from JRH Biosciences (Lenexa, KS, USA). Hoechst 33342, 5,5',6,6'-tetrachloro-1,1',3,3'-tetraethylbenzimidazolyl carbocyanine iodide (JC-1), 5/6-chloromethyl-2',7'-dichlorodihydrofluorescein diacetate acetyl ester (CM-H<sub>2</sub>DCFDA) and dihydroethidium (DHE) were purchased from Invitrogen (Burlington, ON, Canada). H<sub>2</sub>O<sub>2</sub> was diluted to 200  $\mu$ M from a stabilized 30% w/v solution in phosphate buffered saline (PBS) immediately before use. CM-H<sub>2</sub>DCFDA and hemin were initially dissolved in

dimethyl sulfoxide (DMSO) and further diluted in PBS with DMSO  $\leq$ 0.01% as final working concentration. Unless otherwise stated, all other reagents and chemicals were purchased from Sigma-Aldrich (St. Louis, MO, USA).

**Cell Culture.** HL-1 cardiomyocytes were expanded from frozen stocks using Claycomb media supplemented with 10% FBS, 2 mM L-glutamine, 0.1 mM norepinephrine and penicillin/streptomycin (full media) in culture dishes pre-coated with 0.00125% fibronectin and 0.02% gelatin. For experiments, cells were seeded at 5,000/cm<sup>2</sup> and grown to 50% confluence in full media at 37°C in a 95% air:5% CO<sub>2</sub> humidified atmosphere. Prior to experiments, cells were washed twice with PBS and rendered quiescent in Claycomb Minimal Media (0.5% FBS, 2 mM L-glutamine, penicillin/streptomycin; CMM) for 48 hours. Quiescence of HL-1 cells was confirmed by flow cytometric analysis of cell cycle using the DNA-intercalating dye propidium iodide. All experiments were conducted on cells that were passaged at least once after recovery from the frozen stock.

**Quantification of Reactive Oxygen Species Formation.** The non-fluorescent cell permeable probe CM-H<sub>2</sub>DCFDA was used, as described previously (34). Intracellularly this molecule undergoes acetate group removal by intracellular esterases, rendering it membrane-impermeable, and thus is retained in the cytoplasm. Upon oxidation, this molecule becomes fluorescent in proportion to the amount of total non-specific reactive oxygen species generated after exposure to H<sub>2</sub>O<sub>2</sub>. CM-H<sub>2</sub>DCFDA was pre-loaded to cells in 6 well culture dishes at a final concentration of 5  $\mu$ M and incubated for 30 minutes at 37°C. The wells were then washed once with PBS and exposed to 200  $\mu$ M H<sub>2</sub>O<sub>2</sub> in CMM for 45 minutes at 37°C and 5% CO<sub>2</sub>. CM-H<sub>2</sub>DCFDA fluorescence was visualized using epifluorescence at  $\times$ 200 using excitation and emission wavelengths of 480 nm and 520 nm, respectively, and quantified using flow cytometry. To avoid confounding results due to spectral overlap with our GFP controls and CM-H<sub>2</sub>DCFDA, we further assessed oxidative stress by loading the cells with 1  $\mu$ M of the cell permeable DNA intercalating dye dihydroethidium (DHE) for 45 minutes after exposure to H<sub>2</sub>O<sub>2</sub>.

**Induction and Treatments in Cardiomyocyte Hypertrophy Analysis.** Cardiomyocyte hypertrophy was induced by exposing quiescent HL-1 cells to 200  $\mu$ M H<sub>2</sub>O<sub>2</sub> at 0 and 24 hours. Hypertrophy was assessed at 48 hours. For determination of protein synthesis, cells were plated in 24 well culture dishes at 5,000 cells/well. Twenty-four hours after serum starvation, the cells were transduced with 30 multiplicities of infection (MOI) of AdHO-1 or AdGFP for 24 hours. For studies assessing the effect of hemin, bilirubin, CO and N-acetyl cysteine (NAC), the cells were pre-treated with 25  $\mu$ M hemin for 24 hours, 1  $\mu$ M of bilirubin for 1 hour, 10  $\mu$ M of CO releasing molecule (Ru[CO]<sub>3</sub>Cl<sub>2</sub>)<sub>2</sub> or 10 mM NAC prior to and during the addition of H<sub>2</sub>O<sub>2</sub>. For studies assessing the effect of the NF-

$\kappa$ B inhibitor SN50 on H<sub>2</sub>O<sub>2</sub>-induced hypertrophy, cells were pretreated with 4  $\mu$ M of SN50 1 hour prior to and 24 hours after the addition of H<sub>2</sub>O<sub>2</sub>. Forty-two hours after H<sub>2</sub>O<sub>2</sub> treatment, 1  $\mu$ Ci of <sup>3</sup>H-leucine was added to each well for the remaining 6 hours of H<sub>2</sub>O<sub>2</sub> treatment. Protein was collected by 5% trichloroacetic acid precipitation, re-suspended in 1 M sodium hydroxide and analyzed using a liquid scintillation counter (LS 1801; Beckman Coulter Inc.). The radioactivity in each sample was normalized against protein concentration. For planar morphometry determination of cell surface area, cells were digitally photographed using a Retiga EXi Fast 1394 charged-coupled digital camera at  $\times 200$  magnification using the OpenLab software. Three random photographs were taken from each well of 6 well culture plates, and cell surface areas were measured using Adobe Photoshop. A minimum 100 cells were measured for each experimental replicate in a blinded fashion. For visualization of filamentous-actin of the sarcomere, the cells were incubated with phalloidin conjugated to Alexa 594 (Invitrogen) at a dilution of 1:350. Hoechst 33342 was used to counter-stain the nuclei. Images were captured with an inverted fluorescence microscope (Leica Microsystems Inc., Richmond Hill, ON, Canada), using excitation/emission wavelengths of 520 nm/620 nm to visualize phalloidin and 351 nm/364 nm to visualize the nucleus. Images of the same field were overlaid, and the photographs were used to confirm the cell surface measurements obtained by phase-contrast microscopy.

**Transfection of Short-Interfering RNA (siRNA).** Cells were grown in full media until  $\sim 40\%$  confluent, then media was replaced with CMM for 24 hours before transfection, according to supplier recommendations, with 5  $\mu$ g siRNA:3 $\mu$ l Lipofectamine 2000 (Invitrogen) for 6 hours (Double stranded Stealth<sup>TM</sup> siRNA for mouse HO-1 (GGU GGC GAC AGU UGC UGU AGG GCU U-sense; AAG CCC UAC AGC AAC UGU CGC CAC C-anti-sense). Media was removed, washed with PBS, and replaced with CMM for 18 hours prior to treatment with H<sub>2</sub>O<sub>2</sub>, as described.

**Adenoviral Production and Transduction.** The production of the recombinant adenovirus encoding the human HO-1 gene and GFP was prepared using the AdEasy System (Johns Hopkins Oncology Center), as previously described (35). For transduction, HL-1 cardiomyocytes were plated in full media at 50% confluence. Twenty-four hours later, the cells were exposed to 30 MOI of AdHO-1 or AdGFP for 6 hours in CMM. Cells were then washed with PBS, and the media was replaced with fresh CMM. Transduction efficiency was assessed 24 hours after exposure to the virus using flow cytometry and fluorescence microscopy for detection of GFP fluorescence.

**Western Immunoblot Analysis.** Cell lysates were prepared using tissue protein extraction reagent (Pierce, Rockford, IL, USA) containing protease and phosphatase inhibitor cocktails (Sigma). Protein samples (25  $\mu$ g) were

denatured in 4 $\times$  Laemmli buffer and resolved in 10% SDS-PAGE and transferred to polyvinylidene difluoride membrane (0.45 $\mu$ M, Immobilon-P, Millipore, Billerica, MA, USA). HO-1/HO-2 protein was detected using 1:5,000 dilution of a polyclonal antibody (SPA-895/OSA-200, StressGen, Victoria, BC, Canada) and incubated overnight at 4°C. The blots were then incubated with a 1:5,000 dilution of anti-rabbit/mouse HRP-conjugated secondary antibody (#7074/7076, Cell Signaling, Danvers, MA, USA). Immunoreactivity was detected using ChemiGlow (Pierce) and an AlphaEase<sup>TM</sup> gel documentation system (Fluorchem 8900, Alpha Innotech Corp., San Leandro, CA, USA). Membranes were stripped using 0.2 M glycine buffer, pH 2.6, for 1 hour with rocking and re-probed for  $\beta$ -actin (1:5,000; Sigma) for normalization of the data.

**Measurement of HO Enzymatic Activity.** HL-1 cells were washed in 10 mM PBS (pH 7.4), scraped into centrifuge tubes and then centrifuged at  $\times 1,000 g$  for 10 minutes at 4°C. The cell pellet was resuspended in 100 mM PBS (pH 7.4), containing 1 mM ethylenediamine tetraacetic acid disodium, 1 mM phenylmethylsulfonyl fluoride and 10 mg/mL leupeptin. Cells were lysed by sonication on ice; the sonicate was centrifuged at  $\times 12,000 g$  for 15 minutes at 4°C. Total HO activity in the cell lysate was determined by quantitation of CO formed from the degradation of methemalbumin (heme complexed with albumin), according to a published procedure (36). Briefly, reaction mixtures (150  $\mu$ L) consisted of 100 mM phosphate buffer (pH 7.4), 50  $\mu$ M methemalbumin, 0.5–1 mg/mL protein and 1.5 mM  $\beta$ -nicotinamide adenine dinucleotide phosphate, and the incubations were carried out for 30 minutes at 37°C. Reactions were stopped by instantly freezing the reaction mixture on pulverized dry ice, and CO formation was determined by gas chromatography using a TA 3000R Process Gas Analyzer (Trace Analytical, Newark, DE, USA).

**NF- $\kappa$ B Promoter Assay.** Cells were plated in 12 well dishes at 50% confluence in full media. Twenty-four hours after plating, the cells were serum-starved in CMM for 36 hours and then transfected for 12 hours with a NF- $\kappa$ B-luciferase reporter plasmid containing 4 tandem repeats of the NF- $\kappa$ B-DNA binding consensus sequence (a gift from Dr. Aning Lin, University of Chicago, IL). The cells were washed with PBS and treated with 200  $\mu$ M H<sub>2</sub>O<sub>2</sub> for 24 hours. Cells were washed again with PBS and dislodged with HyQtase solution (Hyclone, Logan, UT, USA). The cells were then lysed, and luciferase activity was analyzed in a Lumat LB 9507 luminometer using a BrightGLO<sup>TM</sup> luciferase assay kit from Promega (Madison, WI, USA). To normalize for differences in basal transcriptional rate between the various groups, cells were transfected with a constitutive PGL3-control vector (E1741, Promega) expressing luciferase under the cytomegalovirus (CMV) promoter, and NF- $\kappa$ B promoter activity was subsequently normalized by dividing the corresponding activity of the CMV-promoter activity in each replicate.

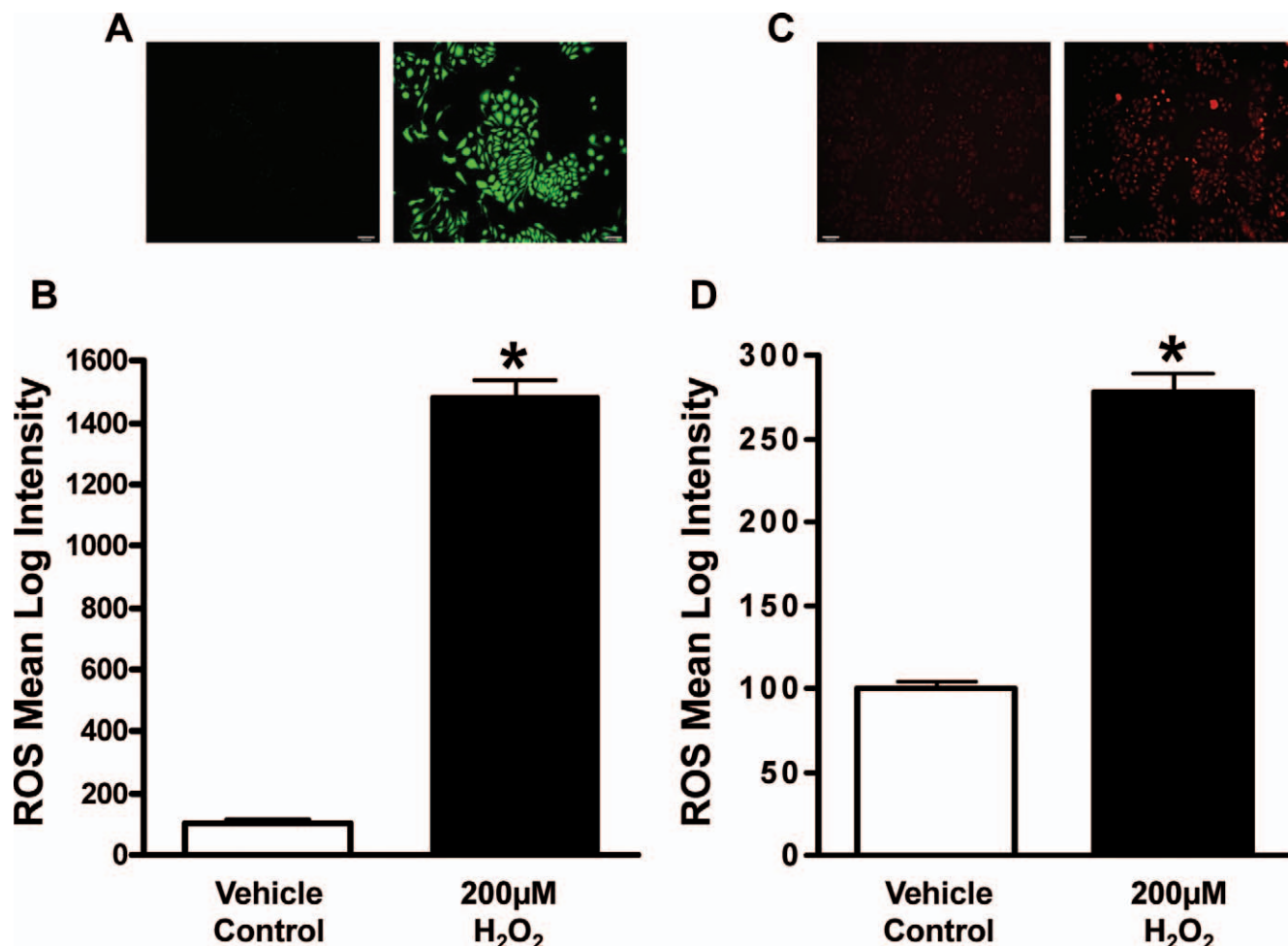


**Figure 1.** Hydrogen peroxide results in perturbed redox imbalance in HL-1 cardiomyocytes. A) Representative images of control (left panel) and 200  $\mu\text{M}$   $\text{H}_2\text{O}_2$  treated HL-1 cardiomyocytes (right panel) using the ROS-sensitive green CM-H<sub>2</sub>DCFDA fluorescence ( $\times 200$ ) and B) mean intensity between two groups. C) Representative images of control (left panel) and 200  $\mu\text{M}$   $\text{H}_2\text{O}_2$  treated HL-1 cardiomyocytes (right panel) using the ROS-sensitive red DHE ( $\times 200$ ). D) Mean intensity of fluorochrome between two groups. (Values are mean  $\pm$  SEM; \*  $P < 0.05$  vs. Vehicle control; FACS analysis was performed in triplicate with a minimum of  $>10,000$  gated cells used to calculate the average log intensity of each replicate in an experiment; the indicated mean is the calculated mean of average log intensities of four independent experiments;  $N = 4$ .)

**NF- $\kappa\text{B}$  Transactivation ELISA.** NF- $\kappa\text{B}$  binding activity was assessed 1 hour after  $\text{H}_2\text{O}_2$  treatment using the NF- $\kappa\text{B}$  NoShift II Transcription Factor ELISA assay (Novagen, Mississauga, ON, Canada) according to the manufacturer's instructions. A total of  $\sim 10$   $\mu\text{g}$  of nuclear protein extract was used for the binding reactions. The luminescence of the samples was measured using a FLUOstar Optima plate reader. The data were normalized for total protein concentration.

**Statistical Analysis.** All results are presented as mean  $\pm$  standard error of the mean (SEM) and displayed as percent change from control, unless otherwise indicated. One-way analysis of variance (ANOVA) followed by Neuman-Keuls multiple comparison test were used for comparisons between the different treatments. A  $P$  value  $< 0.05$  was considered to represent statistical significance.

## Results

**Optimization of HL-1 Model of Oxidant-Induced Cardiomyocyte Hypertrophy.** All experiments were carried out with quiescent HL-1 cardiomyocytes to minimize confounding effects of hyperplastic cell growth. Quiescence of HL-1 myocytes was achieved by maintaining the cells in low serum. Flow cytometric analysis of cell cycle using propidium iodide showed that maintenance of the cells in CMM containing 0.5% FBS decreased the percentage of cycling cells from 62% to 19% after 48 hours (data not shown). Starvation of the cells beyond 48 hours failed to increase the percentage of cells in G<sub>0</sub>/G<sub>1</sub> and reduced cell viability. Thus, all experiments were carried out in cells arrested for 48 hours.

As a step towards optimizing the HL-1 cell culture model of oxidant-induced cardiomyocyte hypertrophy, we determined the concentration of  $\text{H}_2\text{O}_2$  that increased oxidative stress without causing excessive cell death.

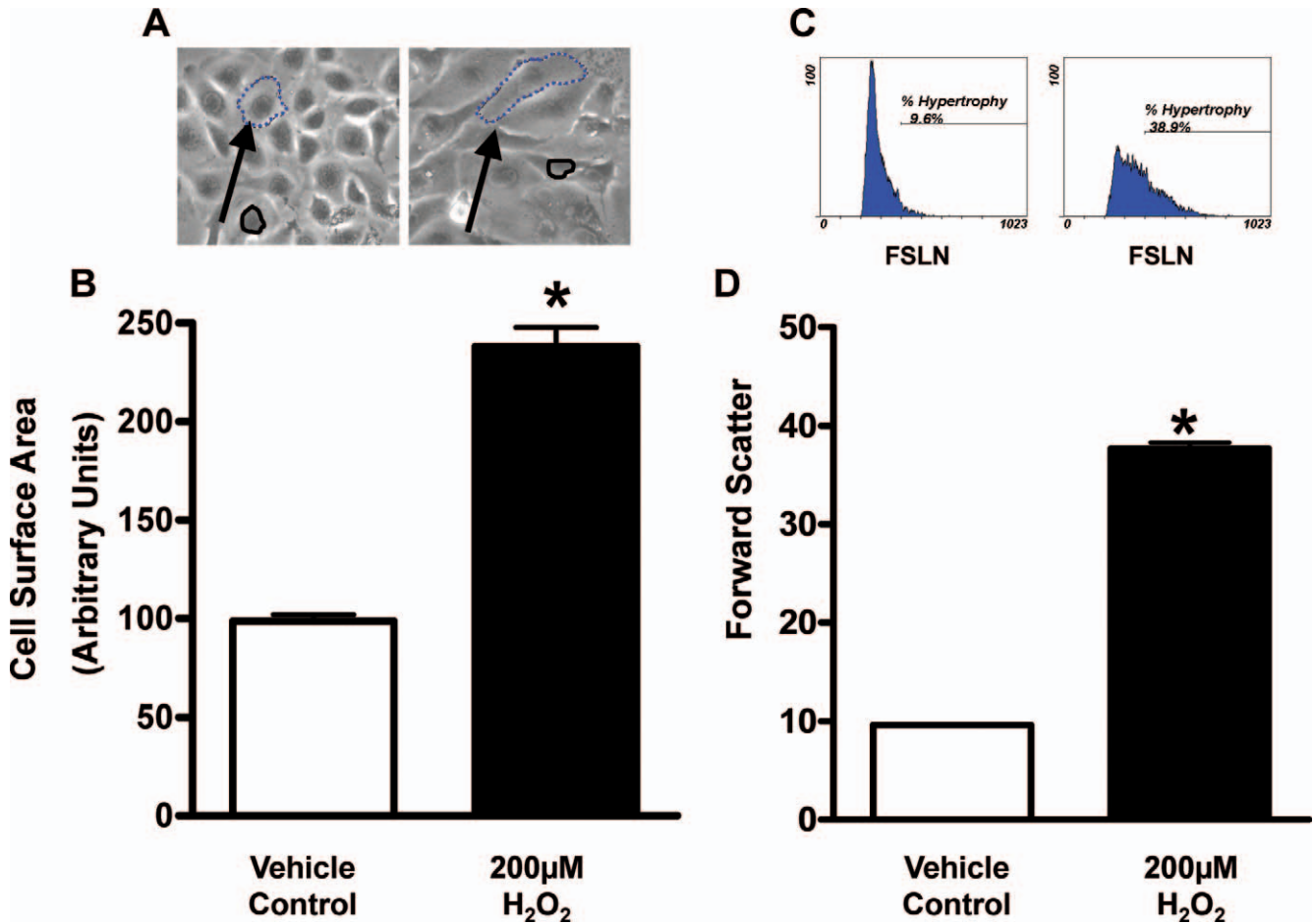


**Figure 2.** Redox imbalance in HL-1 cardiomyocytes results in cellular hypertrophy indicated by increased cell area and cell volume, with no appreciable alteration in nuclear volume. A) Control (left panel) and treated with 200  $\mu\text{M}$   $\text{H}_2\text{O}_2$  (right panel) showing increased cell surface area (dotted lines) with no change in nuclear size (solid lines). B) Increased quantitative planar morphometry between groups. C) Representative forward-scatter histograms of cardiomyocyte cell volume in control (left panel) and treated with 200  $\mu\text{M}$   $\text{H}_2\text{O}_2$  (right panel) values are presented as an increase from control in total Ln-Mean forward scatter. (Values are mean  $\pm$  SEM; \*  $P < 0.05$  vs. Vehicle control; B)  $N =$  mean area of replicates, with  $>100$  cells measured per replicate, total independent experiments are  $N \geq 20$ ; D)  $N =$  average Ln-forward-scatter FACS analysis of  $>10,000$  live gated cells per sample, prepared in triplicate, as before; total independent experiments are  $N = 5$ ).

$\text{H}_2\text{O}_2$  in the range of 50–500  $\mu\text{M}$  produced dose-dependent increases in ROS and hypertrophy as detected by CM- $\text{H}_2\text{DCFDA}$  fluorescence (data not shown). At 200  $\mu\text{M}$ ,  $\text{H}_2\text{O}_2$  increased CM- $\text{H}_2\text{DCFDA}$  fluorescence  $\sim 16$ -fold (Fig. 1A, B). In addition, to avoid confounding results associated with our control adenoviral vectors in the green spectrum, we established a 3-fold increase in ROS with the less promiscuous redox-sensitive dye dihydroethidium (DHE; Fig. 1C, D). Concentrations of  $\text{H}_2\text{O}_2$  beyond 200  $\mu\text{M}$  empirically caused excessive cell death in our culture conditions. Product-stability, exposure-duration and culture-conditions (particularly antioxidants in the media, ie ascorbic acid) of  $\text{H}_2\text{O}_2$  exposure is critical for establishing appropriate physiological ranges. To reaffirm our choice in dose in regard to cell viability we examined early markers of apoptosis and necrosis. The effect of 200  $\mu\text{M}$   $\text{H}_2\text{O}_2$  on mitochondrial membrane potential with the JC-1 and exclusion of propidium iodide confirmed a viable physiologically relevant dose of  $\text{H}_2\text{O}_2$ , since we observed neither

an indication of apoptosomal complex formation by JC-1, nor necrosis resulting in permeability of the cell membrane to propidium iodide (data not shown).

#### Effect of $\text{H}_2\text{O}_2$ on HL-1 Cardiomyocyte Size.

Similar to its effects on ROS generation,  $\text{H}_2\text{O}_2$  induced a dose-dependent increase in cell size in the 50–200  $\mu\text{M}$  (data not shown). Higher concentrations (300–500  $\mu\text{M}$ ) of  $\text{H}_2\text{O}_2$  did not increase cell size any further and, indeed, tended to decrease forward-scatter, likely a consequence of our observed toxicity beyond this range. Therefore, we established 200  $\mu\text{M}$   $\text{H}_2\text{O}_2$  as the optimal, maximal dose as an oxidant threshold to induce hypertrophy. We further examined the effects of hypertrophy in HL-1 cardiomyocytes by measuring changes in cell size (cell surface area) and protein synthesis ( $^3\text{H}$ -leucine incorporation). Exposure of cardiomyocytes to  $\text{H}_2\text{O}_2$  for 48 hours increased cell surface area by 150% (Fig. 2A, B). Comparable to its effects on cell surface area,  $\text{H}_2\text{O}_2$  increased cell size by 3-fold by cytometric forward-scatter analysis (Fig. 2C, D). In

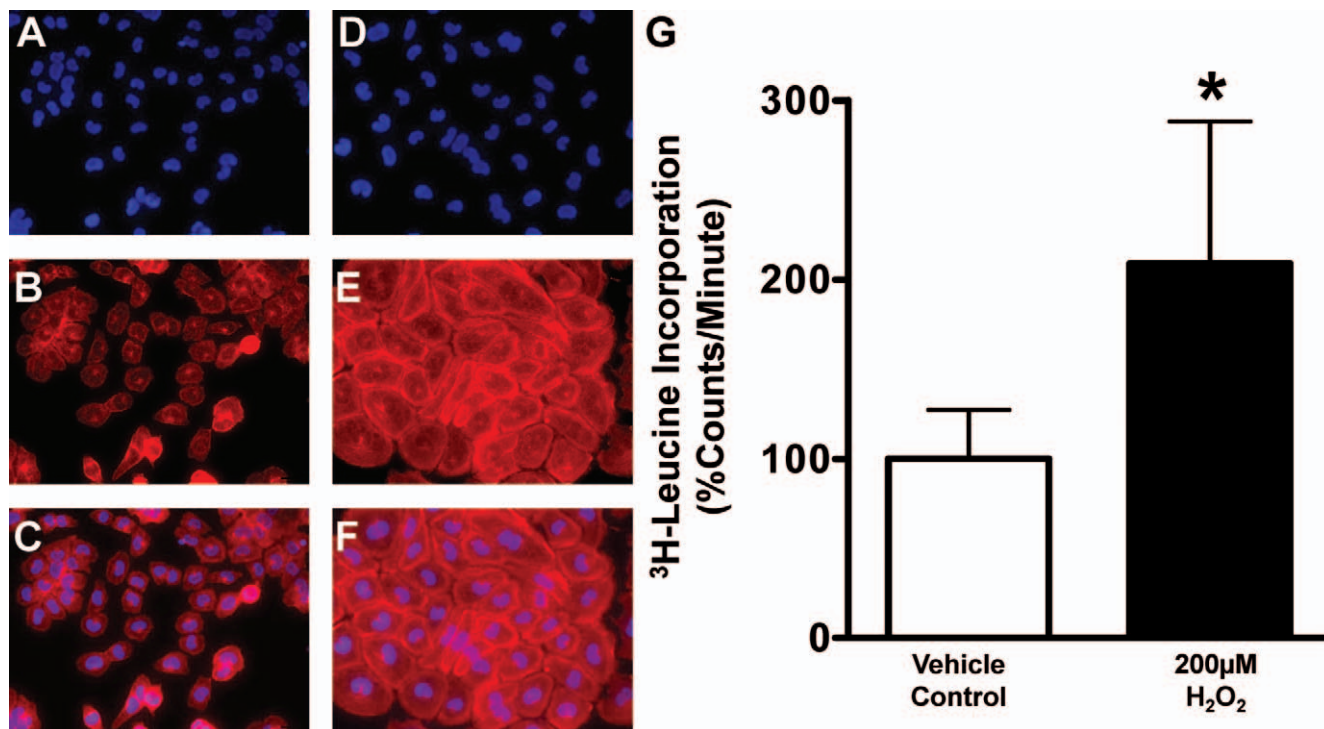


**Figure 3.** HL-1 cardiomyocytes control (A–C) and treated with 200  $\mu\text{M}$   $\text{H}_2\text{O}_2$  (D–F) Hoechst nuclear counterstain (blue A, D) and sarcomeric actin staining by phalloidin (red B, E) with merged images (C, F at  $\times 400$ ) demonstrated abundant protein synthesis of alter phenotype of hypertrophied HL-1 cardiomyocytes. Protein synthesis was further quantified by  $^3\text{H}$ -leucine incorporation (G) as a standardized quantitative index of cellular growth associated with hypertrophy. (Values are mean  $\pm$  SD; \*  $P \leq 0.05$  vs. Vehicle control; G) N = replicates individually normalized to total protein from five independent experiments; N  $\geq 20$ ).

addition, compared to control (Fig. 3A–C), more potent staining of sarcomeric filamentous-actin by phalloidin was observed after treatment with 200  $\mu\text{M}$   $\text{H}_2\text{O}_2$  (Fig. 3D–F). This was accompanied by a general increase in protein synthesis by approximately 100% (Fig. 3G).

**Anti-Hypertrophic Effect of Heme Oxygenase Specific to HO-1 and Its Metabolites via Redox Sensitive Mechanism(s).** Heme oxygenase activity is a product of two enzymes, the inducible isoform HO-1 and

the constitutive isoform HO-2, and both utilize the same substrate, heme. We provided cells with the substrate, heme, prior to exposure to  $\text{H}_2\text{O}_2$  and demonstrated that it could provide an anti-hypertrophic effect (Table 1). This was solely dependent on the presence of HO-1, as knockdown of HO-1 with RNA interference abrogated any benefit. We further established that the major metabolites specific to HO-1, either bilirubin or carbon monoxide, are capable of alleviating oxidant-induced

**Table 1.** HO-1 substrate induction/supply using heme (25  $\mu\text{M}$ ) is able to achieve HO-1 mediated anti-hypertrophic effects, but not without the presence of the enzyme, verifying specificity of HO-1 to the anti-hypertrophic effects mediated by heme oxygenase. Further, the metabolites of heme bilirubin (1 mM) and CO (10 mM) are both able to achieve HO-1 mimetic effects, elucidating a common mediator of hypertrophic growth mediated by HO-1's downstream metabolites, a factor mediated by oxidative stress, since the general antioxidant N-acetylcysteine (NAC) was able to counteract the hypertrophic effects of  $\text{H}_2\text{O}_2$ .

Treatment	$^3\text{H}$ -Leucine incorporation (% counts/minute) <sup>a</sup>
A) Vehicle	100.1 $\pm$ 27.7; n = 39
B) 200 $\mu\text{M}$ $\text{H}_2\text{O}_2$	*209.1 $\pm$ 79.4; n = 19
C) Hemin control	97.6 $\pm$ 19.6; n = 18
D) Hemin + 200 $\mu\text{M}$ $\text{H}_2\text{O}_2$	**107.8 $\pm$ 34.6; n = 18
E) Hemin + RNAi HO1 + 200 $\mu\text{M}$ $\text{H}_2\text{O}_2$	***200.6 $\pm$ 144.1; n = 28
F) Bilirubin + 200 $\mu\text{M}$ $\text{H}_2\text{O}_2$	****113.2 $\pm$ 51.2; n = 7
G) CO + 200 $\mu\text{M}$ $\text{H}_2\text{O}_2$	***97.6 $\pm$ 9.0; n = 6
H) NAC + 200 $\mu\text{M}$ $\text{H}_2\text{O}_2$	****127.7 $\pm$ 69.4; n = 18

<sup>a</sup> Values are mean  $\pm$  SD, n = replicates individually normalized to total protein from two to ten independent experiments.  
\*  $P < 0.001$  vs. Vehicle, \*\*  $P < 0.001$ , \*\*\*\*  $P < 0.01$ , \*\*\*\*  $P < 0.05$  vs.  $\text{H}_2\text{O}_2$ , \*\*\*  $P < 0.001$  vs. Hemin + 200  $\mu\text{M}$   $\text{H}_2\text{O}_2$ .

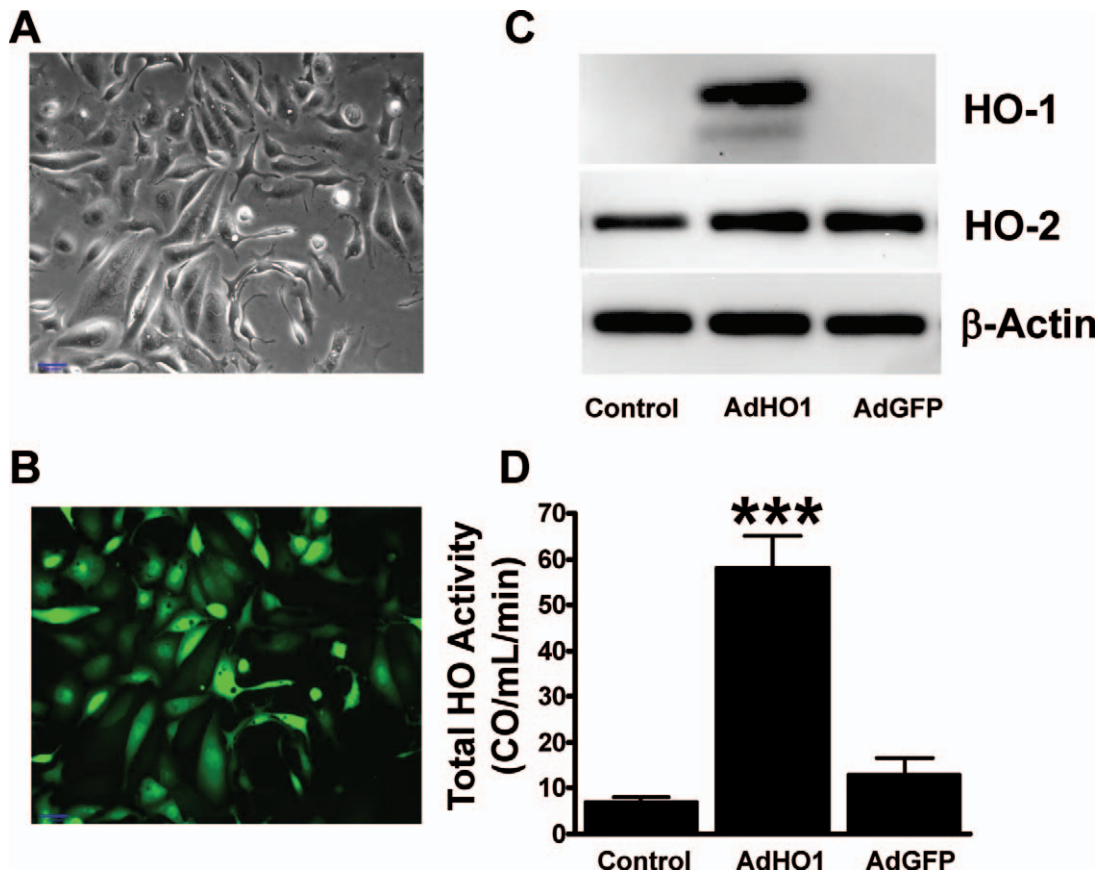


**Figure 4.** Specific expression and activity of HO-1 is achieved using adenoviral vectors. A) Transduction of HO-1 to HL-1 cardiomyocytes (phase) with adenoviral vectors produced >90% transduction efficiency as assessed by (B) GFP green fluorescence ( $\times 200$ ). C) HO-1, HO-2 and Actin Protein expression in untransduced 30MOI AdGFP and AdHO-1 demonstrating high levels of HO-1 protein expression without affecting HO-2. D) HO-1 protein expression corresponds to increased basal HO activity. (Values are mean  $\pm$  SD, results are replicates of a single same day experiment performed in left to right succession of groups; N = 6; \*\*\*  $P \leq 0.001$  vs. Control).

hypertrophy (Table 1). We found these effects to be, in part, redox-dependent, as pre-treatment with the antioxidant N-acetyl cysteine was also able to attenuate oxidant-induced hypertrophy.

**HO-1-Specific Expression Alleviates Oxidant-Induced HL-1 Cardiomyocyte Hypertrophy.** We were able to achieve specific HO-1 expression in HL-1 cardiomyocytes using adenovirus. Transduction efficiency was determined using a control vector that expressed GFP. Post-transduction efficiency was >95%, with 30 MOI of AdGFP at 24 hours (Fig. 4 A,B). HO-1 specific expression was confirmed via western blot with no appreciable difference in HO-2 levels compared to control (Fig. 4C). Basal activity was also determined to be 6-fold higher in HO-1 expressing cells (Fig. 4D). HO-1 expression attenuated the redox imbalance induced by  $H_2O_2$  by  $\sim 60\%$  (Fig. 5A, B). This effect translated to reduced hypertrophic indices, which included a marked reduction in cell size (Fig. 5C), coinciding with an approximately 90% reduction in  $^3H$ -leucine incorporation and cell surface area (Fig. 5D, E).

**The Redox Sensitive Transcription Factor, NF- $\kappa$ B, Mediates Oxidant-Induced Hypertrophy.** We used a luciferase promoter-reporter construct encoding

tandem repeats of the NF- $\kappa$ B consensus sequence to determine the effect of oxidant-induced stimulation of NF- $\kappa$ B promoter activity (Fig. 6A). In addition, we established NF- $\kappa$ B nuclear binding by ELISA. Basal NF- $\kappa$ B promoter binding activity was low in the vehicle treated cells (Fig. 6B). We established that oxidant-induced HL-1 cardiomyocyte hypertrophy was associated with increased NF- $\kappa$ B transactivation through a 3-fold increase in promoter activity (Fig. 6A) and a significant increase in nuclear binding activity (Fig. 6B). The correlation of oxidant-induced NF- $\kappa$ B transactivation was subsequently established as a dependent transcriptional regulator of the oxidant-induced hypertrophic response. Inhibition of NF- $\kappa$ B nuclear translocation with SN-50 abrogates oxidant-induced hypertrophic protein synthesis and increased cell size (Fig. 6C).

**Mechanism of HO-1-Mediated Anti-Hypertrophic Effect via NF- $\kappa$ B.** HO-1 exerts its anti-hypertrophic effects on myocytes by inhibiting the activity of ROS-sensitive factors that block the hypertrophic gene program. Expression of HO-1 reduced NF- $\kappa$ B promoter activity to near basal levels (Fig. 7A). Further examination of the effect of HO-1 overexpression on NF- $\kappa$ B DNA binding activity in response to stimulation with  $H_2O_2$  showed a near 3-fold

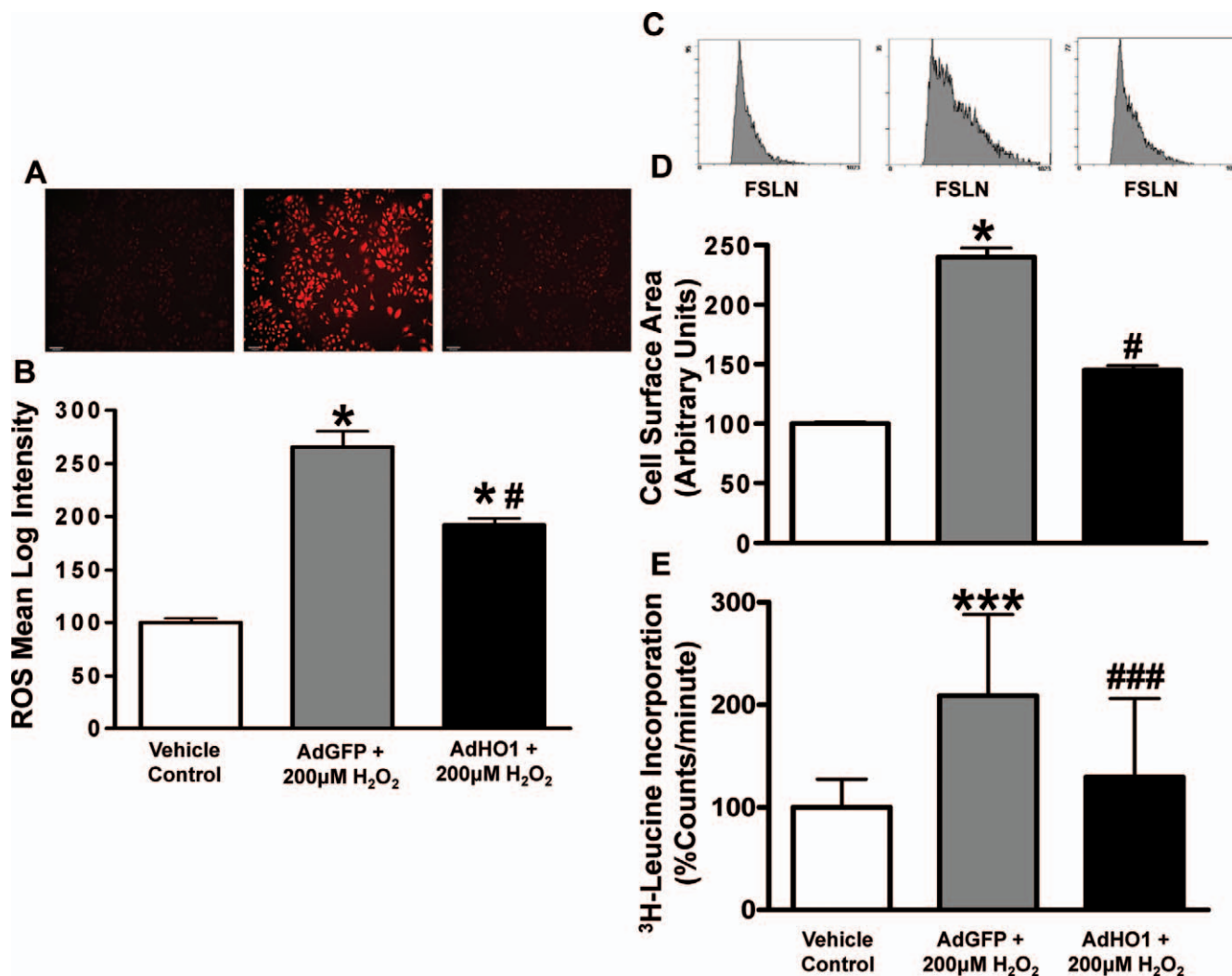


**Figure 5.** HO-1 therapy ameliorates redox imbalance and cellular hypertrophy. A) Representative images of ROS accumulation by DHE in vehicle (left panel), AdGFP treated with 200  $\mu\text{M}$   $\text{H}_2\text{O}_2$  (center panel) and AdHO-1 treated with 200  $\mu\text{M}$   $\text{H}_2\text{O}_2$  (right panel;  $\times 200$ ). B) Mean intensity of fluorochrome; AdHO-1 attenuates ROS accumulation. C) Representative forward scatter histograms of control HL-1 cardiomyocytes (left panel) control vector AdGFP treated with 200  $\mu\text{M}$   $\text{H}_2\text{O}_2$  (center panel) and AdHO-1 treated with 200  $\mu\text{M}$   $\text{H}_2\text{O}_2$  (right panel); AdHO-1 attenuates 200  $\mu\text{M}$   $\text{H}_2\text{O}_2$  induced increase in three dimensional cell size. D) Cell surface area and (E)  $^3\text{H}$ -Lecine incorporation increased by treatment with 200  $\mu\text{M}$   $\text{H}_2\text{O}_2$  in AdGFP is markedly reduced by AdHO-1, respectively. (Values are mean  $\pm$  SEM; \*  $P \leq 0.05$ , \*\*\*  $P \leq 0.001$  vs. Vehicle control, #  $P < 0.05$ , ###  $P \leq 0.001$  vs. AdGFP 200  $\mu\text{M}$   $\text{H}_2\text{O}_2$ ; A–D)  $N =$  mean of triplicate samples for each experiment. Total independent experiments are B)  $N = 4$ ; D)  $N \geq 5$ ; E) Values are mean  $\pm$  SD,  $N =$  replicates individually normalized to total protein from five independent experiments;  $N \geq 20$ ).

reduction in NF- $\kappa\text{B}$  binding in AdHO-1 compared to AdGFP control (Fig. 7B). Combining pre-treatment strategies with SN-50 did not produce additive anti-hypertrophic effects with HO-1 (data not shown). Taken together, these data suggest that oxidant-induced cardiomyocyte hypertrophy is mediated by NF- $\kappa\text{B}$  activation of the hypertrophic gene program and that HO-1 exerts anti-hypertrophic effects, at least in part, by inhibiting NF- $\kappa\text{B}$  activity, via its downstream metabolites to increase the oxidative stress threshold and reduce NF- $\kappa\text{B}$  activity.

## Discussion

Reactive oxygen species (ROS) are continuously generated in the heart as a result of both oxidative

metabolism and enzymatic processes (37) and in response to G-protein coupled receptor activation by agonists (10–12, 38, 39). At low concentrations, ROS participate in cell signaling and in regulation of gene expression (38). Certainly, if ROS pervade in excess, cardiomyocyte apoptotic pathways are activated, in part through regulation of transcription factors such as NF- $\kappa\text{B}$  (40–47). In recent years, ROS have been reported to directly activate many of the signaling pathways involved in cardiac hypertrophy (3, 10–12, 16–18, 38). In the current study, we show that HO-1 overexpression by adenoviral expression markedly reduces cardiomyocyte hypertrophy in response to  $\text{H}_2\text{O}_2$ , a physiologically relevant pro-oxidant species that activates multiple signaling pathways involved in regulation of cardiomyocyte

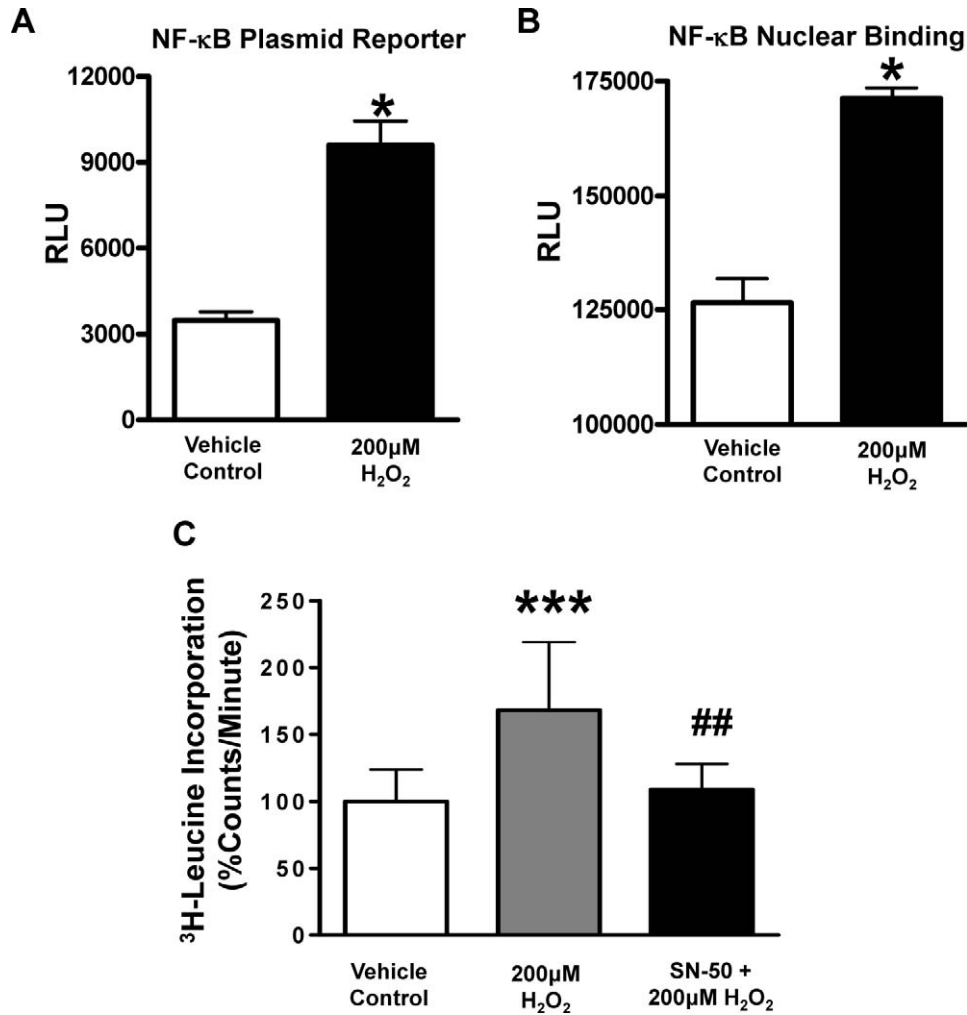


**Figure 6.** Oxidant-induced hypertrophy occurs by an NF-κB transactivation dependent mechanism. A) Four repeats of the NF-κB consensus promoter sequence upstream of a luciferase reporter measured an increase in promoter activation after treatment with 200 μM H<sub>2</sub>O<sub>2</sub>. B) Nuclear protein extract demonstrated active on-target nuclear binding of NF-κB protein after treatment with 200 μM H<sub>2</sub>O<sub>2</sub>. C) Increased <sup>3</sup>H-Leucine incorporation by 200 μM H<sub>2</sub>O<sub>2</sub> is abrogated by inhibition of NF-κB transactivation with an NF-κB translocation inhibitor SN-50. (Values are mean ± SEM; \*  $P \leq 0.05$ , \*\*\*  $P \leq 0.001$  vs. Vehicle control, #  $P \leq 0.05$ , ##  $P \leq 0.01$  vs. 200 μM H<sub>2</sub>O<sub>2</sub>; A–B)  $N =$  mean of duplicate samples as before for each experiment, total independent experiments are A)  $N \geq 8$ ; B)  $N \geq 6$ ; analysis of total samples in B) were performed same day by ELISA from frozen stored isolates; C) Values are mean ± SD,  $N =$  replicates individually normalized to total protein from three independent experiments;  $N = 9$ ).

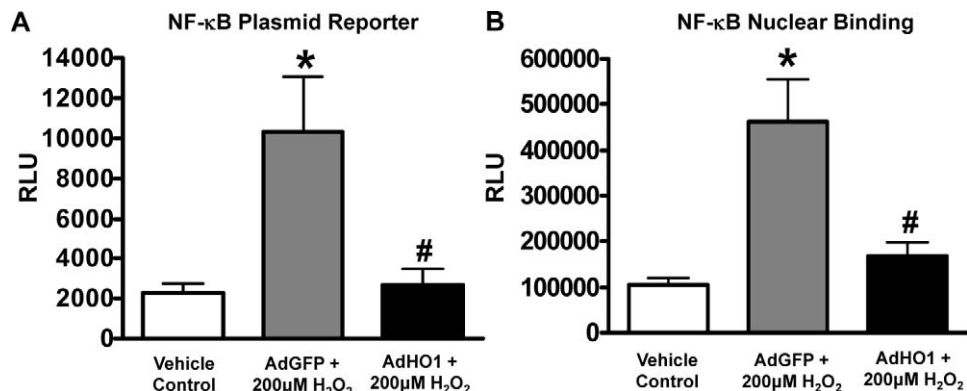


**Figure 7.** Specific expression of HO-1 ameliorates the oxidative stress induced NF-κB transactivation. A) Promoter activity after 200 μM H<sub>2</sub>O<sub>2</sub> is reduced by HO-1 treatment. B) Nuclear protein NF-κB binding activity after 200 μM H<sub>2</sub>O<sub>2</sub> is also reduced by HO-1 treatment. (Values are mean ± SEM; \*  $P \leq 0.05$  vs. Vehicle control, #  $P \leq 0.05$  vs. 200 μM H<sub>2</sub>O<sub>2</sub>;  $N =$  mean of duplicate samples as before for each experiment, total independent experiments are A)  $N \geq 7$ ; B)  $N \geq 15$ ; analysis of B is from frozen isolates and two ELISA sets of the same lot were performed on alternate days for analysis.)

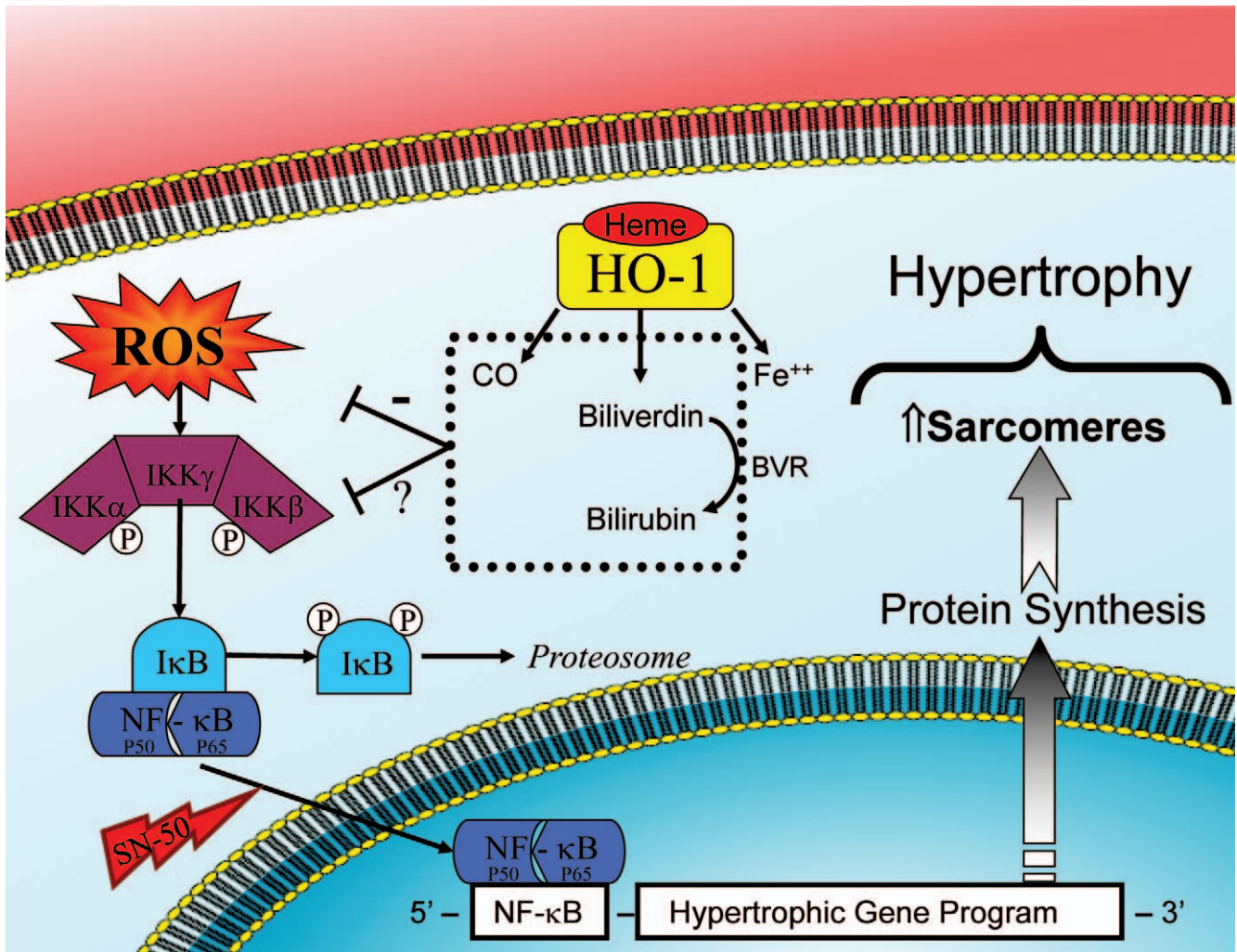


**Figure 8.** Model of HO-1 mediated antihypertrophic effect in HL-1 cardiomyocytes. Redox imbalance in cardiomyocytes activates IKK to phosphorylate IκB, causing its dissociation from NF-κB thereby exposing the nuclear localization signal. Translocation of NF-κB results in the activation of the hypertrophic gene program, thus leading to increased protein synthesis, a consequence related to increased sarcomere formation that ultimately causes cardiomyocyte hypertrophy. HO-1 interrupts this pathway by abrogating NF-κB transactivation, in part through a reduction in excessive ROS accumulation. (HO-1, heme oxygenase-1; BVR, biliverdin reductase; ROS, reactive oxygen species; IKK, IκB kinase; IκB, inhibitor of kappa B; NF-κB, nuclear factor kappa B; SN-50 inhibitor of NF-κB translocation).

growth and apoptosis (40, 41). The anti-hypertrophic effects of HO-1 appear to be mediated, at least in part, via inhibition of NF-κB-dependent transactivation of the hypertrophic gene program. In addition, inhibition of NF-κB nuclear translocation prevents the hypertrophic effect of  $H_2O_2$  in a non-additive manner with HO-1, CO or bilirubin, establishing a convergent mechanism (Fig. 8). This is the first time that HO-1 or its metabolic by-products CO and bilirubin have directly been shown to inhibit oxidant-induced cardiomyocyte hypertrophy by a NF-κB-dependent mechanism, thus supporting the premise that HO-1 is a redox-sensitive negative regulator of cardiomyocyte hypertrophy. Considering the role that ROS play in the pathogenesis of cardiac hypertrophy and heart failure (3–9, 48), the current results suggest strategies aimed at increasing endogenous HO-1 activity may yield therapeutic value for prevention of heart failure.

Previous studies reported that HO-1 overexpression inhibits agonist (phenylephrine, angiotensin II, endothelin 1)-induced hypertrophy of neonatal cardiomyocytes (26, 27). However, in a more recent study, Foo et al (28) reported that HO-1 failed to inhibit angiotensin-induced cardiomyocyte hypertrophy. While, in contrast to our present work, a recent study examining direct oxidant-induced ( $200\mu M H_2O_2$ ) hypertrophy in H9C2 myoblasts demonstrated NF-κB-independent mechanisms (49). Our own studies demonstrate that hemin, a potent inducer and substrate for HO-1, markedly reduces cardiac hypertrophy *in vivo* with pressure overload (50), while others have reported a reduction in arterial blood pressure and heart size in spontaneously hypertensive rats treated with hemin (51). A common feature of these studies is that hypertrophy is accompanied by an increase in ROS generation, and HO-1 may exert its anti-hypertrophic effects by conserving redox

homeostasis. However, a direct effect of HO-1 in this regard has not been previously documented. Our results show that HO-1 inhibits direct oxidant-induced cardiomyocyte hypertrophy through reduced intracellular ROS levels, suggesting that HO-1 exerts its anti-hypertrophic effects, at least in part, by buffering intracellular ROS. In fact, the hypertrophic effect of H<sub>2</sub>O<sub>2</sub> was fully inhibited by pre-treatment with bilirubin, the antioxidant catalytic by-product of heme degradation by HO-1 (22). This suggests that in the presence of adequate substrate-availability, HO-1 over-expression enhances the antioxidant reserve in cardiomyocytes, allowing the cells to cope with increased ROS generation and prevent the activation of ROS-sensitive signaling cascades leading to hypertrophy, apoptosis and heart failure.

The mechanism by which ROS induces the hypertrophic gene program in cardiomyocytes is highly complex, and appears to involve the synchronous activation of multiple upstream kinases (10–12, 14–16) and calcium sensitive pathways, culminating in the activation of redox-sensitive transcription factors such as NF- $\kappa$ B (10–12, 15, 16, 39, 52, 53). Our results indicate that the inhibition of oxidant-induced cardiomyocyte hypertrophy by HO-1 is dependent, at least in part, on inhibition of NF- $\kappa$ B activity (Fig. 8). Interestingly, this link between HO-1 and NF- $\kappa$ B may be selective as an anti-hypertrophic pathway, as previous investigations have demonstrated no link between HO-1 and NF- $\kappa$ B in cardioprotection or preconditioning (54).

NF- $\kappa$ B has been reported to be involved in regulation of cardiomyocyte hypertrophy in response to a variety of stimuli *in vitro* and *in vivo* (38, 55–57). In addition, NF- $\kappa$ B functions cooperatively with other transcription factors involved in regulation of the hypertrophic gene program (52, 58). The common pathway for activation of NF- $\kappa$ B by pro-hypertrophic stimuli appears to be mediated by increased ROS production; however, the mechanism by which ROS activates NF- $\kappa$ B has not been fully characterized (52, 58). Our results clearly demonstrate that NF- $\kappa$ B plays an essential role in ROS-induced hypertrophic signaling, as the effects of H<sub>2</sub>O<sub>2</sub> were completely abolished by SN-50. However, previous investigations have demonstrated that the calcineurin/NFAT pathway is involved in hypertrophic signaling (26). Clearly, these differing conclusions emphasize the heterogeneity of hypertrophic signaling and the need to examine both agonist-induced and oxidant-induced hypertrophic mechanisms. As our study examined the consequences of direct oxidative stress, while others have studied G-protein coupled receptor-mediated mechanisms (26), it may be that the cellular mechanisms are dependent upon the pathological stimulus. Interestingly, the transcriptional regulator p300, a co-regulator in NFAT signalling, and calmodulin kinase IV are both involved in post-translational modifications of the NF- $\kappa$ B subunit p65/RelA (59). The possibility exists for cross-talk or direct interaction between these two vital

transcription factors and should be explored in future studies.

In conclusion, the current study shows for the first time that HO-1 directly inhibits oxidant-induced cardiomyocyte hypertrophy through a NF- $\kappa$ B-mediated mechanism. Since redox imbalance plays a central role in the pathophysiological process leading to cardiac hypertrophy and heart failure, HO-1 may be a suitable therapeutic target for treatment in conditions of hemodynamic overload, such as hypertension, valvular disease and myocardial infarction.

1. Frey N, Olson EN. Cardiac hypertrophy: the good, the bad and the ugly. *Ann Rev Physiol* 65:45–79, 2002.
2. Swynghedauw B. Molecular mechanisms of myocardial remodeling. *Physiol Rev* 79:215–262, 1999.
3. Giordano FJ. Oxygen, oxidative stress, hypoxia and heart failure. *J Clin Invest* 115:500–508, 2005.
4. Sawyer DB, Siwik DA, Xiao L, Pimentel DR, Singh K, Colucci WS. Role of oxidative stress in myocardial hypertrophy and failure. *J Mol Cell Cardiol* 34:379–388, 2002.
5. Lang D. Cardiac hypertrophy and oxidative stress: a leap of faith or stark reality? *Heart* 87:316–318, 2002.
6. Dhalla AK, Singal PK. Antioxidant changes in hypertrophied and failing guinea pig hearts. *Am J Physiol* 266:H1280–H1285, 1994.
7. Nakamura K, Fushimi K, Kouchi H, Mihara K, Miyazaki M, Ohe T, Namba M. Inhibitory effects of antioxidants on neonatal rat cardiac myocyte hypertrophy induced by tumor necrosis factor- $\alpha$  and angiotensin. *Circulation* 98:794–799, 1998.
8. Date M, Morita T, Yamamshita N, Nishida K, Yamaguchi O, Higuchi Y, Hirotsu S, Matsumura Y, Hori M, Tada M, Otsu K. The antioxidant N-2-mercaptopyropionyl glycine attenuates left ventricular hypertrophy in *in vivo* murine pressure-overload model. *J Am Coll Cardiol* 39:907–912, 2002.
9. Kinugawa S, Tsutsui H, Hayashidani S, Ide T, Suematsu N, Satoh S, Utsumi H, Takeshita A. Treatment with dimethylthiourea prevents left ventricular remodeling and failure after experimental myocardial infarction in mice: role of oxidative stress. *Circ Res* 87:392–398, 2000.
10. Tu VC, Bahl JJ, Chen QM. Signals of oxidant-induced cardiomyocyte hypertrophy: key activation of p70 S6 Kinase-1 and phosphoinositide 3-kinase. *J Pharmacol Exp Ther* 300:1101–1110, 2002.
11. Tanaka K, Honda M, Takabatake T. Redox regulation of MAPK pathways and cardiac hypertrophy in adult rat cardiac myocyte. *J Am Coll Cardiol* 37:676–685, 2001.
12. Xiao L, Pimentel DR, Wang J, Singh K, Colucci WS, Sawyer DB. Role of reactive oxygen species and NAD(P)H oxidase in  $\alpha_1$ -adrenoceptor signaling in adult rat cardiac myocytes. *Am J Physiol* 282:C926–C934, 2002.
13. Higuchi Y, Otsu K, Nishida K, Hirotsu S, Nakayama H, Yamaguchi O, Matsumura Y, Ueno H, Tada M, Hori M. Involvement of reactive oxygen species-mediated NF- $\kappa$ B activation in TNF- $\alpha$  induced cardiomyocyte hypertrophy. *J Mol Cell Cardiol* 34:233–240, 2002.
14. Kwon SH, Pimentel DR, Remondino A, Sawyer DB, Colucci WS. Hydrogen peroxide regulates cardiac myocyte phenotype via concentration-dependent activation of distinct kinase pathways. *J Mol Cell Cardiol* 35:615–621, 2003.
15. Pimentel DR, Amin JK, Xiao L, Miller T, Viereck J, Oliver-Krasinski J, Baliga R, Wang J, Siwik DA, Singh K, Pagano P, Colucci WS, Sawyer DB. Reactive oxygen species mediates amplitude-dependent hypertrophic and apoptotic responses to mechanical stretch in cardiac myocytes. *Circ Res* 89:453–460, 2001.
16. Takano H, Zou Y, Hasegawa H, Akazawa H, Nagai T, Komuro I. Oxidative stress-induced signal transduction pathways in cardiac

- myocytes: Involvement of ROS in heart diseases. (2003) *Antiox Redox Signal* 5:789–794, 2003.
17. Sabri AB, Hughie HH, Lucchesi PA. Regulation of hypertrophic and apoptotic signaling pathways by reactive oxygen species in cardiac myocytes. *Antiox Redox Signal* 5:731–740, 2003.
  18. Yamamoto M, Yang G, Hong C, Liu J, Holle E, Yu X, Wagner T, Vatner SF, Sadoshima J. Inhibition of endogenous thioredoxin in the heart increases oxidative stress and cardiac hypertrophy. *J Clin Invest* 112:1395–1406, 2003.
  19. Kawano S, Kubota T, Monden Y, Kawamura N, Tsutsui H, Takeshita A, Sunagawa K. Blockade of NF-kappaB ameliorates myocardial hypertrophy in response to chronic infusion of angiotensin II. *Cardiovasc Res* 67(4):689–698, 2005.
  20. Ryter SW, Alam J, Choi AMK. Heme oxygenase/carbon monoxide: From basic science to therapeutic application. *Physiol Rev* 86:583–650, 2006.
  21. Stocker RY, Yamamoto Y, McDonagh AF, Glazer AN, Ames BN. Bilirubin is an antioxidant of possible physiological significance. *Science* 235:1043–1046, 1987.
  22. Otterbein LE, Bach FH, Alam J, Soares M, Lu HT, Wysk M, Davis RJ, Flavell RA, Choi AM. Carbon monoxide has anti-inflammatory effects involving the mitogen-activated protein kinase pathway. *Nat Med* 6: 422–428, 2000.
  23. Sharma HS, Maulik N, Gho BCG, Das DK, Verdouw PD. Coordinated expression of heme oxygenase-1 and ubiquitin in the porcine heart subjected to ischemia and reperfusion. *Mol. Cell. Biochem* 157:111–116, 1996.
  24. Melo LG, Agrawal R, Zhang L, Rezvani M, Mangi AA, Ehsan A, Griese DP, Dell'Acqua G, Mann MJ, Oyama J, Yet SF, Layne MD, Perrella MA, Dzau VJ. Gene therapy strategy for long-term myocardial protection using adeno-associated virus-mediated delivery of heme oxygenase gene. *Circulation* 105:602–607, 2002.
  25. Yet SF, Tian R, Layne MD, Wang ZY, Maemura K, Solovyeva M, Ith B, Melo LG, Zhang L, Ingwall JS, Dzau VJ, Lee ME, Perrella MA. Cardiac-specific expression of heme oxygenase-1 protects against ischemia and reperfusion injury in transgenic mice. *Circ Res* 89:168–173, 2001.
  26. Tongers J, Fiedler B, König D, Kempf T, Klein G, Heineke J, Kraft T, Gambaryan S, Lohmann SM, Drexler H, Wollert KC. Heme oxygenase-1 inhibition of MAP kinases calcineurin/NFAT signaling, and hypertrophy in cardiac myocytes. *Cardiovasc Res* 63:545–552, 2004.
  27. Hu CM, Chen YH., Chiang MT, Chau LY. Heme oxygenase-1 inhibits angiotensin-II-induced cardiac hypertrophy in vitro and in vivo. *Circulation* 110:309–316, 2004.
  28. Foo RSY, Siow RCM, Brown MJ, Bennett MR. Heme oxygenase-1 gene transfer inhibits angiotensin II-mediated rat cardiac myocyte apoptosis but not hypertrophy. *J Cell Physiol* 209:1–7, 2006.
  29. Claycomb WC, Lanson Jr N, Stallworth BS, Egeland DB, Delcarpio JB, Bahinski A, Izzo NJ. HL-1 cells: A cardiac muscle cell line that contracts and retains phenotypic characterization of the adult cardiomyocyte. *Proc Natl Acad Sci USA* 95:2979–2984, 1998.
  30. White SM, Constantin PE, Claycomb WC. Cardiac physiology at the cellular level: use of cultured HL-1 cardiomyocytes for studies of cardiac muscle cell structure and function. *Am J Physiol* 286:823–829, 2004.
  31. Clément SA, Tan CC, Guo J, Kitta K, Suzuki YJ. Roles of protein kinase C and alpha-tocopherol in regulation of signal transduction for GATA-4 phosphorylation in HL-1 cardiac muscle cells. *Free Radic Biol Med* 32(4):341–349, 2002.
  32. Kitta K, Clément SA, Remeika J, Blumberg JB, Suzuki YJ. Endothelin-1 induces phosphorylation of GATA-4 transcription factor in the HL-1 atrial-muscle cell line. *Biochem J* 359:375–380, 2001.
  33. Chandrasekar B, Mummidi S, Claycomb WC, Mestrlil R, Nemer M. Interleukin-18 is a pro-hypertrophic cytokine that acts through a phosphatidylinositol 3-kinase-phosphoinositide-dependent kinase-1-Akt-GATA4 signaling pathway in cardiomyocytes. *J Biol Chem* 280: 4553–4657, 2005.
  34. Brunt KR, Fenrich KK, Kiani G, Tse MY, Pang SC, Ward CA, Melo LG. Protection of human vascular smooth muscle cells from H2O2-induced apoptosis through functional codependence between HO-1 and AKT. *Arterioscler Thromb Vasc Biol* 26(9):2027–2034, 2006.
  35. Liu XM, Chapman GB, Wang H, Durante W. Adenovirus-mediated heme oxygenase-1 gene expression stimulates apoptosis in vascular smooth muscle cells. *Circulation* 105:79–84, 2002.
  36. Cook MN, Nakatsu K, Mark GS, McLaughlin BE, Vreman, HJ, Stevenson DK, Brien JF. Heme oxygenase activity in the adult rat aorta and liver as measured by carbon monoxide formation. *Can J Physiol Pharmacol* 73:515–518, 1995.
  37. Droge W. Free radicals in the physiological control of cell function. *Physiol Rev* 82:47–95, 2002.
  38. Freund C, Schmidt-Ulrich R, Baurand A, Dunger S, Schneider W, Loser P, El-Jamali A, Dietz R, Scheidereit C, Bergmann MW. Requirement of nuclear factor kappaB in angiotensin II- and isoproterenol-induced cardiac hypertrophy in vivo. *Circulation* 111:2319–2325, 2005.
  39. Aikawa R, Komuro I, Yamazaki T, Zou Y, Kudoh S, Tanaka M, Shiojima I, Hiroi Y, Yazaki Y. Oxidative stress activates extracellular signal-regulated kinases through Src and Ras in cultured cardiac myocytes of neonatal rats. *J Clin Invest* 100:1813–1821, 1997.
  40. Zechner D, Craig R, Hanford DS, McDonough PM, Sabbadini RA, Glembotski CC. MKK6 activates myocardial cell NF-kappaB and inhibits apoptosis in a p38 mitogen-activated protein kinase-dependent manner. *J Biol Chem* 273(14):8232–8239, 1998.
  41. Adderley SR, Fitzgerald DJ. Oxidative damage of cardiomyocytes is limited by extracellular regulated kinases 1/2-mediated induction of cyclooxygenase-2. *J Biol Chem* 274(8):5038–5046, 1999.
  42. Craig R, Larkin A, Mingo AM, Thuerauf DJ, Andrews C, McDonough PM, Glembotski CC. p38 MAPK and NF-kappa B collaborate to induce interleukin-6 gene expression and release. Evidence for a cytoprotective autocrine signaling pathway in a cardiac myocyte model system. *J Biol Chem* 275(31):23814–23824, 2000.
  43. Frantz S, Kelly RA, Bourcier T. Role of TLR-2 in the activation of nuclear factor kappaB by oxidative stress in cardiac myocytes. *J Biol Chem* 276(7):5197–5203, 2007.
  44. Craig R, Wagner M, McCardle T, Craig AG, Glembotski CC. The cytoprotective effects of the glycoprotein 130 receptor-coupled cytokine, cardiotrophin-1, require activation of NF-kappa B. *J Biol Chem* 276(40):37621–37629, 2001.
  45. Regula KM, Ens K, Kirshenbaum LA. IKK beta is required for Bcl-2-mediated NF-kappa B activation in ventricular myocytes. *J Biol Chem* 277(41):38676–38682, 2002.
  46. Kumar A, Herald WC, Michael P, Brabant D, Parissenti AM, Ramana CV, Xu X, Parrillo JE. Human serum from patients with septic shock activates transcription factors STAT1, IRF1, and NF-kappaB and induces apoptosis in human cardiac myocytes. *J Biol Chem* 280(52): 42619–42626, 2005.
  47. Rhee SG. H2O2, a necessary evil for cell signaling. *Science* 312:1882–1883, 2006.
  48. Takimoto E, Kass DA. Role of oxidative stress in cardiac hypertrophy and remodeling. *Hypertension* 49:241–248, 2007.
  49. Gupta MK, Neelakantan TV, Sanghamitra M, Tyagi RK, Dinda A, Maulik S, Mukhopadhyay CK, Goswami SK. An assessment of the role of reactive oxygen species and redox signaling in norepinephrine induced apoptosis and of H9c2 cardiac myoblasts *Antiox Redox Signal* 8(5–6):1081–1093, 2006.
  50. Liu XL, Murduck J, Tsuji M, Tse Y, Pang SC, Melo LG. Exogenous heme oxygenase-1 induction reduces cardiac hypertrophy in response to aortic coarctation: Implications for treatment of heart failure. *FASEB J* 19:Abstract #709.11, 2005.
  51. Ndisang JF, Zhao W, Wang R. Selective regulation of blood pressure

- by heme oxygenase-1 in hypertension. *Hypertension* 40:315–321, 2002.
52. Gloire G, Legrand-Poels S, Piette J. NF- $\kappa$ B activation by reactive oxygen species: Fifteen years later. *Biochem Pharmacol* 72:1493–1505, 2006.
53. Ha T, Li Y, Gao X, McMullen JR, Shioi T, Izumo S, Kelley JL, Zhao A, Haddad GE, Williams DL, Browder IW, Kao RL, Li C. Attenuation of cardiac hypertrophy by inhibiting both mTOR and NF $\kappa$ B activation in vivo. *Free Radic Biol Med*. 39:1570–1580, 2005.
54. Das S, Fraga CG, Das DK. Cardioprotective effect of resveratrol via HO-1 expression involves p38 map kinase and PI-3-kinase signaling, but does not involve NF $\kappa$ B. *Free Radic Res* 40(10):1066–1075, 2006.
55. Purcell NH, Tang G, Yu C, Mercurio F, DiDonato JA, Lin A. Activation of NF- $\kappa$ B is required for hypertrophic growth of primary rat neonatal ventricular cardiomyocytes. *Proc Natl Acad Sci U S A* 98: 6668–6673, 2001.
56. Li Y, Ha T, Gao X, Kelley J, Williams DL, Browder IW, Kao RL, Li C. NF- $\kappa$ B activation is required for the development of cardiac hypertrophy in vivo. *Am J Physiol* 287:H1712–H1720, 2004.
57. Hirotani S, Otsu K, Nishida K, Higuchi Y, Morita T, Nakayama H, Yamaguchi O, Mano T, Matsumura Y, Ueno H, Tada M, Hori M. Involvement of nuclear factor- $\kappa$ B and apoptosis signal-regulating kinase 1 in G-protein-coupled receptor agonist-induced cardiomyocyte hypertrophy. *Circulation* 105:509–515, 2002.
58. Jones WK, Brown M, Ren X, He S, McGuinness M. NF- $\kappa$ B as an integrator of diverse signaling pathways: the heart of myocardial signaling. *Cardiovasc Toxicol* 3:229–254, 2003.
59. Hall G, Hasday JD, Rogers TB. Regulating the regulator: NF- $\kappa$ B signaling in heart. *J Mol Cell Cardiol*. 41(4):580–591, 2006.